

Journal of Materials Chemistry A

Accepted Manuscript



This is an *Accepted Manuscript*, which has been through the Royal Society of Chemistry peer review process and has been accepted for publication.

Accepted Manuscripts are published online shortly after acceptance, before technical editing, formatting and proof reading. Using this free service, authors can make their results available to the community, in citable form, before we publish the edited article. We will replace this *Accepted Manuscript* with the edited and formatted *Advance Article* as soon as it is available.

You can find more information about *Accepted Manuscripts* in the [Information for Authors](#).

Please note that technical editing may introduce minor changes to the text and/or graphics, which may alter content. The journal's standard [Terms & Conditions](#) and the [Ethical guidelines](#) still apply. In no event shall the Royal Society of Chemistry be held responsible for any errors or omissions in this *Accepted Manuscript* or any consequences arising from the use of any information it contains.

CO₂-stable reduction-tolerant Nd-containing dual phase membrane for oxyfuel CO₂ capture

Cite this: DOI: 10.1039/x0xx00000x

Huixia Luo,^{a,b*} Tobias. Klande,^a Zhengwen Cao,^a Fangyi Liang,^a Haihui Wang,^{c*} and Jürgen Caro^{a*}

Received 00th January 2012,
Accepted 00th January 2012

DOI: 10.1039/x0xx00000x

www.rsc.org/

Here we report a novel CO₂-stable reduction-tolerant dual-phase oxygen transport membrane with a composition of 40 wt.% Nd_{0.6}Sr_{0.4}FeO_{3-δ}-60 wt.% Ce_{0.9}Nd_{0.1}O_{2-δ} (40NSFO-60CNO), which was successfully developed by facile one-pot EDTA-citric sol-gel method. The microstructure of the crystalline 40NSFO-60CNO phase was investigated by combined in-situ X-ray diffraction (XRD), scanning electron microscopy (SEM), back scattered SEM (BSEM), and energy dispersive X-ray spectroscopy (EDXS). Oxygen permeation and long-time stability under CO₂ and CH₄ atmospheres were investigated. A stable oxygen flux of 0.21 cm³min⁻¹cm⁻² at 950 °C with undiluted CO₂ as sweep gas is found which is increased to 0.48 cm³min⁻¹cm⁻² if the air side is coated with a porous La_{0.6}Sr_{0.4}CoO_{3-δ} (LSC) layer. All the experimental results demonstrate that the 40NSFO-60CNO not only shows a good reversibility of the oxygen permeation fluxes upon temperature cycling, but also good phase stability in a CO₂ atmosphere and under the harsh conditions of the partial oxidation of methane to synthesis gas up to 950 °C.

Introduction

Mixed ionic-electronic conducting oxygen transport materials (OTMs) offer high potential applications as cathode in solid oxide fuel cells (SOFCs),^{1,2} as membrane or adsorbent for oxygen production from air or other oxygen containing gases, or in membrane reactors for the partial hydrocarbon oxidation.³⁻⁶ A challenging application of OTMs would be the oxyfuel process with integrated CO₂ capture.^{7,8} However, to survive under real process conditions in the presence of harsh gases (such as CO₂, H₂, CH₄, etc) at high temperatures, a dense oxygen separation membrane should possess the following properties: (i) high oxygen permeation fluxes; (ii) good structural stability within appropriate ranges of temperature and oxygen partial pressure; (iii) sufficient chemical compatibility and mechanical strength.⁹

The state-of-the-art OTMs are mostly oxygen deficient perovskites containing Ba and/or Sr on the A-site and Co/Fe on the B-site since these cations match the perovskite lattice (Goldschmidt's tolerance factor¹⁰), but also because of their low manufacturing cost, simple design and high oxygen ion transport rates.¹¹⁻¹³ Even though these perovskite-type OTMs show high oxygen permeation fluxes, their poor thermo-mechanical strength, their low chemical stability, and their unsatisfied long-term stability under CO₂/SO₂ atmospheres or at low oxygen partial pressure are still the major barriers for a widespread application.¹⁴⁻¹⁶ Especially, most of the single phase perovskite-type OTMs contain high basicity alkaline-earth ions,

and are, therefore, susceptible to carbonate formation in a CO₂ containing atmosphere.¹⁷⁻¹⁹

Recently, some dual phase composite membranes, which consist of an oxygen ionic conducting (OIC) phase and an electronic conducting (EC) phases in a micro-scale phase mixture, have been developed and exhibit high steady oxygen permeation in CO₂ atmospheres, such as NiFe₂O₄-Ce_{0.9}Gd_{0.1}O_{2-δ},^{7,20} Fe₂O₃-Ce_{0.9}Gd_{0.1}O_{2-δ},²¹ Mn_{1.5}Co_{1.5}O_{4-δ}-Ce_{0.9}Pr_{0.1}O_{2-δ},²² SmMn_{1.5}Co_{1.5}O_{4-δ}-Ce_{0.9}Sm_{0.1}O_{2-δ},²³ Ba_{0.5}Sr_{0.5}Fe_{0.2}Co_{0.8}O_{3-δ}-Ce_{0.9}Gd_{0.1}O_{2-δ},²⁴ La_{0.9}Sr_{0.1}FeO_{3-δ}-Ce_{0.9}Sm_{0.1}O_{2-δ}²⁵ et al. However, some problems still exist; for instance, (a) the easily to reduce Co and/or Ni metal ions in the EC phase with a large dependence of the ionic radius on the valence state which is unfavorable for the membrane stability under a large oxygen concentration gradient;^{7,20-23} (b) Chemical compatibility and stability of the two phases by blocked cation diffusion between the two phases.²⁵

It is known that the oxygen permeation and stability properties of dual phase membrane depend strongly on their electronic and ionic conductivity, on the chemical compatibility, and phase and chemical stability. Therefore, based on our previous studies on dual phase membranes,²⁰⁻²² here we design a novel cobalt-free noble-metal free CO₂-stable and reduction-tolerant dual phase membrane material, 40wt.%Nd_{0.6}Sr_{0.4}FeO_{3-δ}-60wt.% Ce_{0.9}Nd_{0.1}O_{2-δ} (abbreviated as 40NSFO-60CNO). In this dual phase system, CNO is the main OIC phase, and NSFO is the main EC phase for electronic transport. However, the latter phase NSFO also assists the oxygen ionic transport. The basic idea for choosing this system is as follows: (i)

The Fe-based perovskite oxides (e.g Fe-doped Ln (Ln= La series elements) SrO_3) are reported to show a higher stability than Co/Ni-based oxides under a reducing or CO_2 atmosphere²⁶ and show good p-type electronic conductivity.^{27,28} (ii) In a recent study, covering a large number of 10 at.% rare earth doped cerias, synthesized under similar conditions, Nd-doping ceria is reported to exhibit the highest ionic conductivity.²⁹ (iii) Based on the common ion effects, which was defined as the suppression of dissociation of a weak electrolyte containing a common ion, we chose the same element (Nd) in both OIC and EC phases in order to reduce the element diffusion between the two phases;³⁰ (iv) The concentration of the highly EC component NSFO in the dual phase materials was chosen to be 40 wt.% in order to guarantee a continuous electron transport in a percolation network.

Therefore, the aim of this study is the development of a 40NSFO-60CNO dual phase membrane via a facile one-pot EDTA-citric method. The phase structure and stability as well as oxygen permeation have been investigated under different atmospheres (especially CO_2 and CH_4) at high temperatures.

Experimental

Preparation of powders and membranes

The 40wt.% $\text{Nd}_{0.6}\text{Sr}_{0.4}\text{FeO}_{3.8}$ -60wt.% $\text{Ce}_{0.9}\text{Nd}_{0.1}\text{O}_{2.8}$ (40NSFO-60CNO) dual phase powder mixture was synthesized via a facile in-situ one-pot EDTA-citric acid method. The appropriate stoichiometric metal nitrates $\text{Sr}(\text{NO}_3)_2$, $\text{Fe}(\text{NO}_3)_3$, $\text{Ce}(\text{NO}_3)_3$ and $\text{Nd}(\text{NO}_3)_3$ in aqueous solutions were mixed in a beaker. After stirring for 20 min, the calculated amounts of citrate and EDTA were added and the pH value was adjusted to ~ 9 by ammonia. The molar ratio of citric acid: EDTA: total metal ions was 1.5:1:1. Then the solutions were stirred while heated to 150 °C, until the water was evaporated and a gel has been formed. The gels were calcined in air at 600 °C in a furnace to remove the organic compounds by combustion, and the primary powders were obtained. The resulting powders were calcined at 950 °C for 10 h in air. The 40NSFO-60CNO powders were pressed to disk membranes under a pressure of 5 MPa in a stainless steel module with a diameter of 18 mm to get green disk membranes. These green disks were pressure-less sintered at 1400 °C in air for 5 h in air. The surfaces of the disks were carefully polished to 0.60 mm thickness by using 1200 grit-sand paper (average particle diameter 15.3 μm), then the membranes were washed with ethanol.

Characterization of membranes

The phase structure of the dual phase membranes after sintering at 1400 °C for 5 h in air was determined by X-ray diffraction (XRD, using a D8 Advance, Bruker-AXS, with Cu $K\alpha$ radiation, $\lambda = 1.5418 \text{ \AA}$). Data sets were recorded at room temperature in a step-scan mode in the 2θ range of 20° - 80° with intervals of 0.02°. In-situ XRD was conducted in a high-temperature cell HTK-1200N (Anton-Paar) from 30 °C to 1000 °C. The in-situ XRD tests in air and a 50 vol. % CO_2 /50 vol. % N_2 atmosphere were performed with a heating rate of 12 °C/min. At each temperature step, the sample was hold for 50 minutes for thermal equilibrium before diffraction data collection. The disc membranes were studied by scanning electron microscopy (SEM) using a JEOL JSM-6700F at an excitation voltage of 20 keV. The element distribution in the grains of the fresh dual phase membranes under study was investigated on the same electron microscope by energy dispersive X-ray spectroscopy (EDXS), Oxford Instruments INCA-300 EDX spectrometer with an ultra-thin window at an excitation voltage of 20 keV.

Oxygen permeation performances of membranes

The oxygen permeation was studied in a home-made high-temperature oxygen permeation permeator, which is described in a previous paper.³¹ The disc membranes were sealed onto a quartz tube at 950 °C for 5 hours with a gold paste (Heraeus, Germany), the side wall of the membrane disc was also covered with the gold paste to avoid any radial contribution to the oxygen permeation flux. The effective areas of the membranes for oxygen permeation were 0.785 cm^2 . Air as feed gas was fed into one side of the membrane and He or CO_2 as sweep gases were fed into the other side of the membrane. All the inlet gas flow rates were controlled by gas mass flow controllers (Bronkhorst, Germany) and all flow rates were regularly calibrated by using a bubble flow meter. Synthetic air (20 % O_2 and 80 % N_2) with a flow rate of 150 $\text{cm}^3 \text{ min}^{-1}$ was the feed; a mixture of He or CO_2 (49 $\text{cm}^3 \text{ min}^{-1}$) and Ne (1 $\text{cm}^3 \text{ min}^{-1}$) as the internal standard gas was fed to the sweep side. An Agilent 6890A gas chromatograph with a Carboxen 1000 column was employed to analyze the gas mixture. All of disks were carefully polished with 1200 mesh sandpaper from both sides to achieve a 0.6 mm membrane thickness. Before oxygen permeation, both surfaces of the polished disks were cleaned with ethanol. To improve the oxygen surface exchange rate on the air side, the 40NSFO-60CNO membrane was coated with a $\text{La}_{0.6}\text{Sr}_{0.4}\text{CoO}_{3.8}$ (LSC) porous layer, which shows a good oxygen reducing activity when it acts as cathode materials for SOFC.³² After coating with the LSC layer, the membrane was calcined at 950 °C for 2 h.

In addition, the 40NSFO-60CNO dual phase membrane has been used as a membrane reactor for POM. The membrane reactor configuration for POM was described elsewhere.³³ A Ni-based catalyst (0.3 g, Süd Chemie AG) was loaded on the top of the membrane disc and then the temperature of the reactor was increased to 950 °C with a heating rate of 2 °C min^{-1} . All gas lines to the reactor and the gas chromatograph were heated to 180 °C. High-purity methane with He dilution was used as the reactant for the POM to synthesis gas. Gas composition was analyzed by an online gas chromatograph (GC, Agilent 6890A).

Results and discussion

Characterization of the 40NSFO-60CNO dual phase material

The XRD patterns of the as-obtained NSFO, CNO, 40NSFO-60CNO powders calcined at 950 °C for 10 h in air and of the 40NSFO-60CNO dual phase membrane sintered at 1400 °C for 5 h in air, are shown in Fig. 1c. From the XRD, it can be concluded that both the calcined dual phase powder and the sintered membranes are composed of only the cubic fluorite CNO phase (see Fig. 1a, space group 225, Fm3m) and the orthorhombic distorted perovskite NSFO (see Fig. 1b, space group 74, Imma). Table 1S summarizes the lattice parameters of NSFO and CNO as pure phases, in the 40NSFO-60CNO dual phase powder, and in the 40NSFO-60CNO dual phase membrane. It was found that the lattice parameters of the pure CNO and NSFO phases are similar in the 40NSFO-60CNO dual phase powder and in the sintered membrane. The lattice volume of CNO in the 40NSFO-60CNO composite powders is also similar to the single CNO powder. There are no additional phases (such as NdFeO_3 and NdSrFeO_4) even though the dual phase mixture was prepared by a facile one-pot EDTA-citric sol-gel method, which indicate a good chemical compatibility between the two phases NSFO and CNO. Fig. 2 presents the SEM, BSEM and EDXS pictures of the as-prepared 40NSFO-60CNO dual phase membrane after sintering at 1400 °C for 5 h in air at two different magnifications before

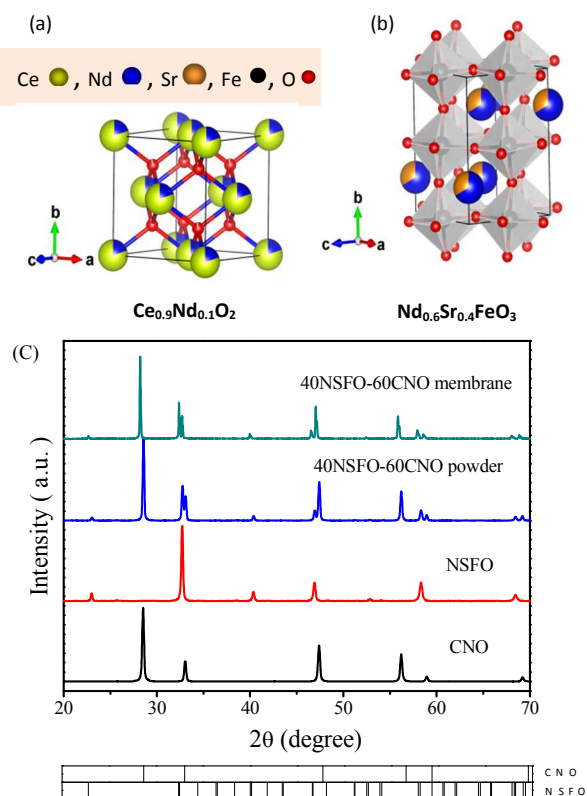


Fig. 1 (a) Structure of (a) cubic fluorite $\text{Ce}_{0.9}\text{Nd}_{0.1}\text{O}_2$ (CNO), and (b) orthorhombic distorted perovskite $\text{Nd}_{0.6}\text{Sr}_{0.4}\text{FeO}_3$ (NSFO); (c) XRD patterns of CNO, NSFO and the dual phase 40NSFO-60CNO powder calcined at 950 °C for 10 h and the 40NSFO-60CNO dual phase membrane sintered at 1400 °C for 5 h.

polishing. SEM images (Fig. 2a, b) revealed that the micro-sized grains are packed closely. The CNO and NSFO grains are distributed very uniformly in the membrane; no major cracks are visible. In the bulk only a few non-connected pores were observed. The NSFO and CNO grains could be distinguished by BSEM and EDXS (Fig. 2c-f). The dark grains in BSEM are NSFO and the light ones CNO, since the contribution of the backscattered electrons to the SEM signal intensity is proportional to the atomic number. The same information is provided by EDXS (Fig. 2e, f), which suggests that the green color (dark in the black-and-white version) is an overlap of the Nd, Fe and Sr signals, whereas the yellow color (light) stems from an average of the Ce and Nd signals. The average grain size areas of NSFO and CNO have been estimated to $0.157 \mu\text{m}^2$ and $0.210 \mu\text{m}^2$ from the analysis of 130 grains, respectively. The STEM and EDXS mappings shown in Fig. 1S indicate that the membrane consists of a micro-scale mixture of well-separated NSFO (mixed ion-electron conductor) and CNO (oxygen ions conductor) grains forming a percolation network.

Phase stability of the 40NSFO-60CNO dual phase material

Fig. 3a shows the in-situ XRD patterns of the sintered 40NSFO

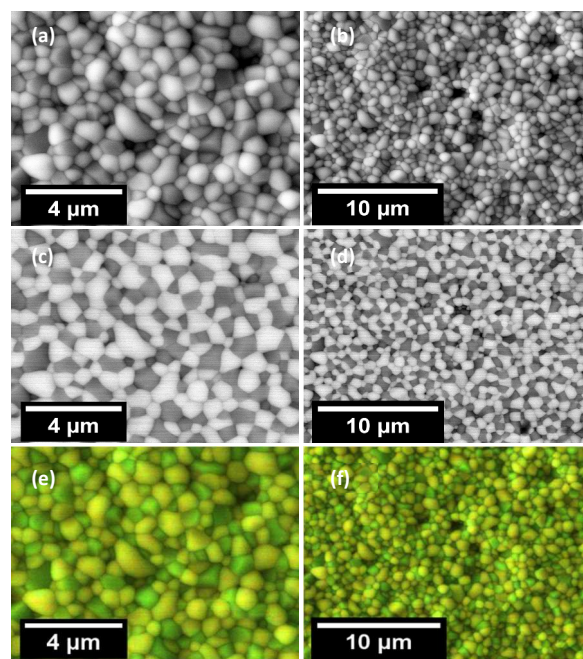


Fig. 2 SEM (a,b), BSEM (c,d), and EDXS (e,f) images of the 40NSFO-60CNO membrane after sintered at 1400 °C for 5 h in air before polishing (see Figure 1). For the EDXS mapping in Figure 3e,f, superimpositions of the Nd $L\alpha$, Sr $K\alpha$ and Fe $K\alpha$ (green) and Nd $L\alpha$ and Ce $L\alpha$ (yellow) have been used.

-60CNO dual phase membrane after crashed into powder, collected in air with increasing temperature from 30 °C to 1000 °C. During heating, no additional reflexes except those of NSFO and CNO phases were observed, suggesting that the phases of CNO and NSFO remain unchanged in the 40NSFO-60CNO dual phase material. Additionally, the high-temperature phase stability in a CO_2 containing atmosphere has been studied by in-situ XRD (Fig. 3b) between 30 °C and 1000 °C in an atmosphere of 50 vol.% CO_2 and 50 vol.% N_2 . As can be seen from Fig. 3b, the dual phase membrane completely keeps its two phases of NSFO and CNO. CO_2 is known to be a sensitive gas to most of the single phase perovskite OTM materials which especially contain high basicity element such as Ba. On the other hand, it has been reported that a phase transition occurs at moderate and high temperatures in the Co-containing single phase perovskite OTM materials, also for some dual phase membranes.^{26,34} However, no carbonate formation or phase transition could be observed in our dual phase membrane 40NSFO-60CNO in an atmosphere of 50 vol.% CO_2 and 50 vol.% N_2 in the temperature range of 30 °C and 1000 °C suggesting that the dual phase membrane 40NSFO-60CNO is thermally and chemically stable both in air and in CO_2 up to 1000 °C. The long-time stability of the oxygen flux with pure CO_2 as sweep gas also confirmed the stability of our dual-phase membrane in CO_2 (Fig. 6).

Oxygen permeation and chemical stability under CO_2

Fig. 4 shows the oxygen permeation flux through the 40NSFO-60CNO dual phase membrane as a function of temperature with pure He and CO_2 as sweep gases with/without $\text{La}_{0.6}\text{Sr}_{0.4}\text{CoO}_{3-\delta}$ (LSC)

porous layer coating of the 40NSFO-60CNO. All the data were collected after the oxygen permeation has reached a steady state (after about 20 h.). The reason for this experimental finding maybe is related to the oxygen exchange reactions on the gas–solid interface of the membranes. The gas–solid interface exchange is slow because of the dense and small membrane surface area. On the other hand, the steady time is related to the dual phase material or composition ratio. This behaviour has been reported in many dual phase membrane, such as x wt.% Fe_2O_3 - $(100-x)$ wt.% $\text{Ce}_{0.9}\text{Gd}_{0.1}\text{O}_{2-\delta}$ ($x = 25, 40, 50$),²¹ 40 wt.% $\text{Pr}_{0.6}\text{Sr}_{0.4}\text{Co}_{0.5}\text{Fe}_{0.5}\text{O}_{3-\delta}$ - 60 wt.% $\text{Ce}_{0.9}\text{Pr}_{0.1}\text{O}_{2-\delta}$,³⁴ 25 wt.% $\text{Sm}_{0.6}\text{Sr}_{0.4}\text{FeO}_{3-\delta}$ - 75 wt.% $\text{Ce}_{0.85}\text{Sm}_{0.15}\text{O}_{1.925}$.³⁵ As shown in Fig. 4a, the oxygen permeation fluxes through all of our dual phase membranes increase with increasing temperature. For the dual phase membrane without LSC coating, oxygen permeation fluxes of 0.26 and 0.21 $\text{cm}^3 \text{min}^{-1} \text{cm}^{-2}$ are found at 950 °C for the pure sweep gases He and CO_2 . On the other hand, it was found that when the temperature increases from 850 °C to 950 °C, the oxygen permeation flux through the membrane with a LSC porous layer coating on the air side increases from 0.21 $\text{cm}^3 \text{min}^{-1} \text{cm}^{-2}$ to a stable

value of 0.48 $\text{cm}^3 \text{min}^{-1} \text{cm}^{-2}$ for a membrane thickness of 0.6 mm, when CO_2 has been used as a sweep gas. The 40CNO-60NSFO dual phase membrane shows lower oxygen permeation flux than most of the single perovskite membrane for He as a sweep gas in comparison with literature data (Table 1). However, when using CO_2 as a sweep gas, the oxygen permeation flux is much higher than reported for the single phase and other dual phase oxygen permeable membranes and even higher than those of some Co-containing dual phase membranes.³⁶

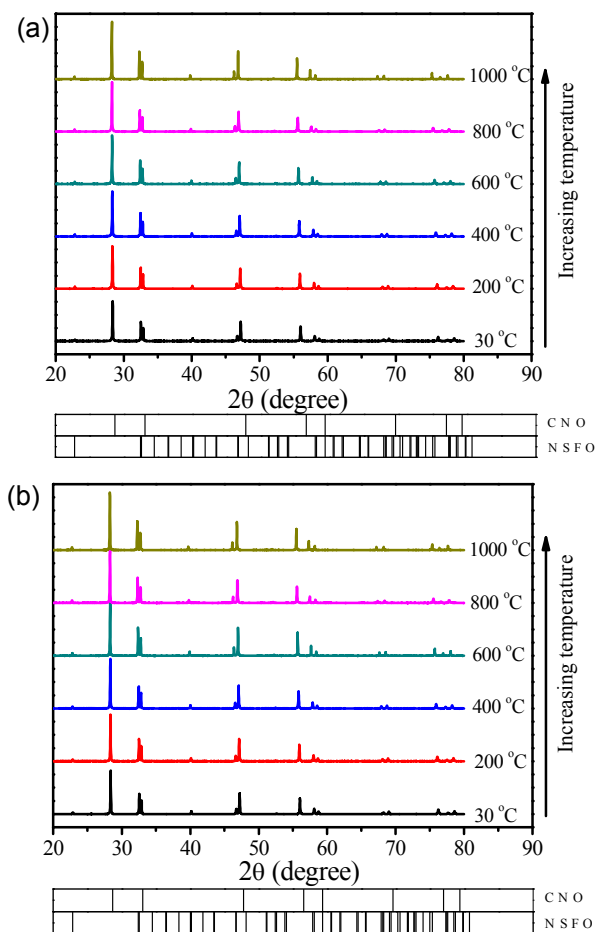


Fig. 3 In-situ XRD patterns of the 40NSFO-60CNO dual phase membrane sintered at 1400 °C for 5 h after crashed for increasing temperature in (a) air and (b) in 50 vol.% CO_2 and 50 vol.% N_2 . Conditions: Heating rate = 12 °C·min⁻¹; equilibration time at each temperature: 50 min for recording the XRD data at each temperature; $F_{\text{total}} = 100 \text{ cm}^3 \text{min}^{-1}$.

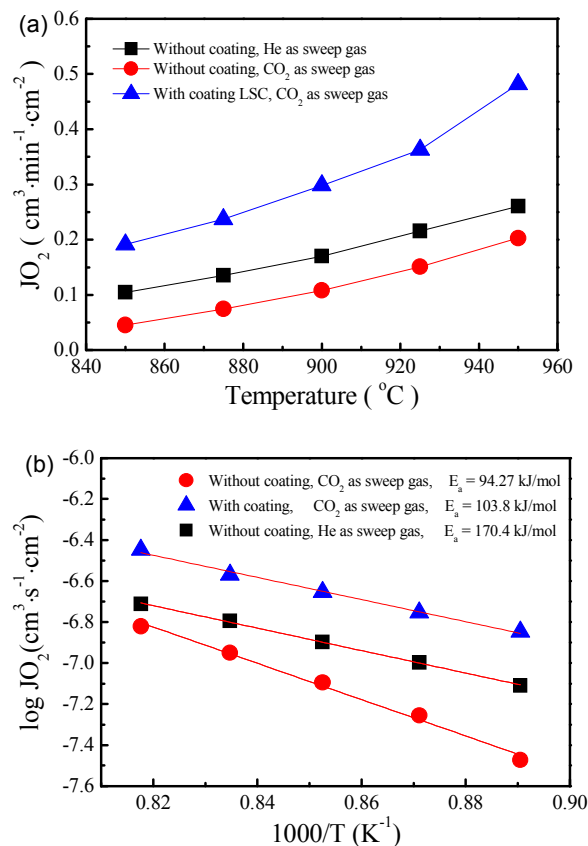


Fig. 4 Oxygen permeation flux through 40NSFO-60CNO dual phase membrane as a function of temperature with pure He/ CO_2 as sweep gas for membranes without and with porous $\text{La}_{0.6}\text{Sr}_{0.4}\text{CoO}_{3-\delta}$ (LSC) coating on the air side.

Conditions: 150 $\text{cm}^3 \text{min}^{-1}$ air as feed gas, 49 $\text{cm}^3 \text{min}^{-1}$ He/ CO_2 as sweep gas; 1 $\text{cm}^3 \text{min}^{-1}$ Ne as internal standard gas. Membrane thickness: 0.6 mm.

Furthermore, the Arrhenius plot (Fig. 4b) indicates that oxygen permeation can be described by a single apparent activation energy in the temperature range of 850 - 950 °C with pure CO_2 as the sweep gas. It has been suggested that the change of activation energy is caused by the change in rate-controlling process.^{22,37,38} Here, the fluorite phase is the main phase in the dual-phase system. And the oxygen permeation flux for the LSC coating 40CNO-60NSFO dual phase membrane is two times higher than that of the uncoated coating membrane (see Fig. 6). The rate-limiting step of oxygen

ARTICLE

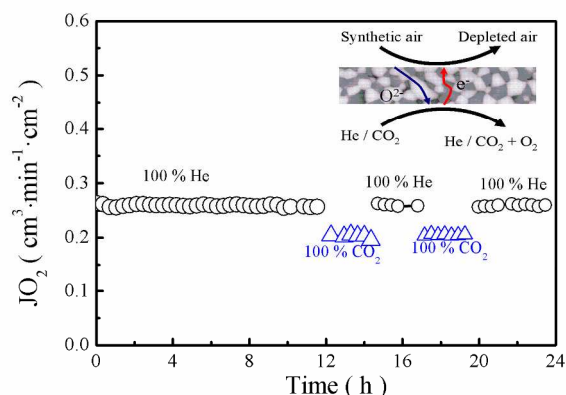
Table 1. Steady-state oxygen permeation flux (J_{O_2}) through different OTM membranes in disk geometries.

Membrane materials	Thickness (mm)	Temperature ($^{\circ}\text{C}$)	Oxygen flux ($\text{cm}^3 \text{min}^{-1} \cdot \text{cm}^{-2}$) Air/He	Oxygen flux ($\text{cm}^3 \text{min}^{-1} \cdot \text{cm}^{-2}$) Air/ CO_2	Ref.
a) $\text{Ba}_{0.5}\text{Sr}_{0.5}\text{Co}_{0.8}\text{Fe}_{0.2}\text{O}_{3-\delta}$	1	875	1.9	0	16
a) $\text{La}_{0.5}\text{Sr}_{0.5}\text{Co}_{0.8}\text{Fe}_{0.2}\text{O}_{3-\delta}$	1	900	-	0.1	25
a) $\text{La}_{0.9}\text{Sr}_{0.1}\text{FeO}_{3-\delta}$	1	1000	0.22	-	24
a) 40wt.% NiFe_2O_4 -60wt.% $\text{Ce}_{0.9}\text{Gd}_{0.1}\text{O}_{2-\delta}$	0.5	950	0.18	0.16	6,18
a) 40wt.% Fe_2O_3 -60wt.% $\text{Ce}_{0.9}\text{Gd}_{0.1}\text{O}_{2-\delta}$	0.5	950	0.10	0.08	19
a) 40wt.% $\text{Mn}_{1.5}\text{Co}_{1.5}\text{O}_{4-\delta}$ -60wt.% $\text{Ce}_{0.9}\text{Pr}_{0.1}\text{O}_{2-\delta}$	0.5	1000	0.22	0.20	22
a) 40wt.% $\text{Pr}_{0.6}\text{Sr}_{0.4}\text{FeO}_{3-\delta}$ -60wt.% $\text{Ce}_{0.9}\text{Pr}_{0.1}\text{O}_{2-\delta}$	0.6	950	0.27	0.18	8
b) 25wt.% $\text{Sm}_{0.6}\text{Ca}_{0.4}\text{CoO}_{3-\delta}$ -75wt.% $\text{Ce}_{0.8}\text{Sm}_{0.2}\text{O}_{2-\delta}$	0.5	950	0.23	0.16	36
a) 40wt.% $\text{Nd}_{0.6}\text{Sr}_{0.4}\text{FeO}_{3-\delta}$ -60wt.% $\text{Ce}_{0.9}\text{Nd}_{0.1}\text{O}_{2-\delta}$	0.6	950	0.26	0.21	This work
c) 40wt.% $\text{Nd}_{0.6}\text{Sr}_{0.4}\text{FeO}_{3-\delta}$ -60wt.% $\text{Ce}_{0.9}\text{Nd}_{0.1}\text{O}_{2-\delta}$	0.6	950	-	0.48	This work

a): Both sides of membrane uncoated with $\text{La}_{0.6}\text{Sr}_{0.4}\text{CoO}_{3-\delta}$ porous layer;

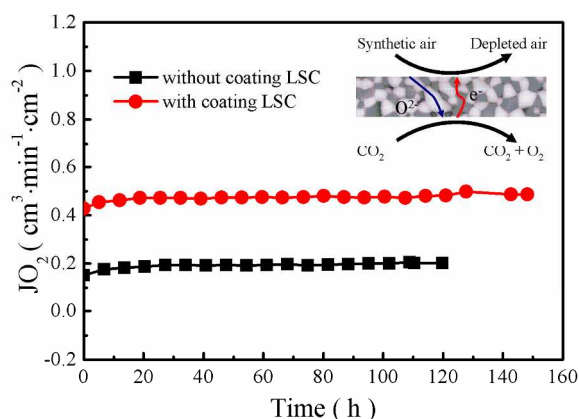
b): Both sides of membrane coated with 25wt.% $\text{Sm}_{0.6}\text{Ca}_{0.4}\text{CoO}_{3-\delta}$ - 75wt.% $\text{Ce}_{0.8}\text{Sm}_{0.2}\text{O}_{2-\delta}$ porous layer;

c): Air side of membrane coated with $\text{La}_{0.6}\text{Sr}_{0.4}\text{CoO}_{3-\delta}$ porous layer.

**Fig. 5** Oxygen permeation fluxes as function of time while periodically changing the sweep gas.

Conditions: $150 \text{ cm}^3 \text{ min}^{-1}$ air as feed gas, $49 \text{ cm}^3 \text{ min}^{-1}$ He and $1 \text{ cm}^3 \text{ min}^{-1}$ Ne or $49 \text{ cm}^3 \text{ min}^{-1}$ CO_2 and $\text{cm}^3 \text{ min}^{-1}$ Ne as sweep gas; Membrane thickness: 0.6 mm. Temperature: $950 \text{ }^{\circ}\text{C}$. Without LSC coating.

permeation through 40CNO-60NSFO maybe is related to oxygen surface exchange. However, determination of which of the limiting transport in the 40CNO-60NSFO dual phase membrane was not performed. Further investigation will be studied in future. Meanwhile, it is accepted that a single activation energy is an important indication that there is no phase transformation in the membrane under study.³⁹ This conclusion is in agreement with the finding that the oxygen flux with pure CO_2 as a sweep gas is found to be long-time stable (see Fig. 6).

**Fig. 6** Oxygen permeation flux through 40NSFO-60CNO dual phase membrane as a function of time with pure CO_2 as sweep gas for membranes without and with porous LSC coating

Conditions: $150 \text{ cm}^3 \text{ min}^{-1}$ air as feed gas, $49 \text{ cm}^3 \text{ min}^{-1}$ CO_2 as sweep gas; $1 \text{ cm}^3 \text{ min}^{-1}$ Ne as internal standard gas. Membrane thickness: 0.6 mm. Temperature: $950 \text{ }^{\circ}\text{C}$.

Fig. 5 shows the reversibility of the oxygen permeation flux through the 40NSFO-60CNO membrane without LSC coating when periodically changing the sweep gas between He and CO_2 at $1000 \text{ }^{\circ}\text{C}$. When using He as a sweep gas, a stable oxygen permeation flux of $0.26 \text{ cm}^3 \text{ min}^{-1} \text{ cm}^{-2}$ can be obtained, whereas the oxygen permeation flux decreases immediately to the slightly lower value of $0.21 \text{ cm}^3 \text{ min}^{-1} \text{ cm}^{-2}$, if CO_2 instead of He is used as the sweep gas. This behavior was also observed in the previous studies of a CO_2 -stable dual phase membrane which is ascribed to the slight inhibiting effect of CO_2 on the oxygen surface-exchange. This behaviour is

different to previous findings on the perovskite-type membranes containing high basicity alkaline-earth metals (such as Ba) e.g. $\text{Ba}_{0.5}\text{Sr}_{0.5}\text{Co}_{0.8}\text{Fe}_{0.2}\text{O}_{3-\delta}$ (BSCF),¹⁷ $\text{BaCo}_x\text{Fe}_y\text{Zr}_z\text{O}_{3-\delta}$ (BCFZ),¹⁸ and $\text{Ba}(\text{Co}_{0.4}\text{Fe}_{0.4}\text{Nb}_{0.2})\text{O}_{3-\delta}$,¹⁹ where the oxygen permeation flux decreases sharply due to the formation of carbonates if CO_2 was present. But the chemical stability of perovskite-type membrane material strongly depends on A and/or B-site composition as well. Thus, the primary approach used to improve the CO_2 stability of the perovskite-type materials is to modify the composition by doping other metals into the perovskite structure. It has been reported that CO_2 -tolerant materials (such as $\text{La}_{0.6}\text{Sr}_{0.4}\text{Co}_{0.8}\text{Fe}_{0.2}\text{O}_{3-\delta}$,^{26,40,41} $\text{La}_{0.6}\text{Ca}_{0.4}\text{Co}_{0.8}\text{Fe}_{0.2}\text{O}_{3-\delta}$ ⁴²) can be obtained by doping less basicity alkaline-earth metal or non-alkaline earth metals (such as La, Ca).⁴⁰⁻⁴³ In our study the 40NSFO-60CNO membrane has good reversibility of the oxygen permeation fluxes and good chemical stability in a CO_2 atmosphere.

The time dependence of the oxygen permeation flux through the 40NSFO-60CNO dual phase composite membrane with and without LSC coating for CO_2 as sweep gas is shown in Fig. 6 During the whole oxygen permeation, an oxygen permeation flux for the uncoated and coated membrane is about $0.21 \text{ cm}^3 \text{ cm}^{-2} \text{ min}^{-1}$ and $0.48 \text{ cm}^3 \text{ cm}^{-2} \text{ min}^{-1}$ respectively at $1000 \text{ }^\circ\text{C}$ and no decrease with time was found. Combing the in-situ XRD, the reversibility of the oxygen permeation measurements when switching the sweep gases from CO_2 to He, and the stable oxygen permeation fluxes on our 40NSFO-60CNO, we can exclude chemical reactions between the two NSFO and CNO phases involved like reported in previous studies of dual phase membranes.^{7,8,20,21}

40NSFO-60CNO membrane reactor in the partial oxidation of methane (POM) to synthesis gas

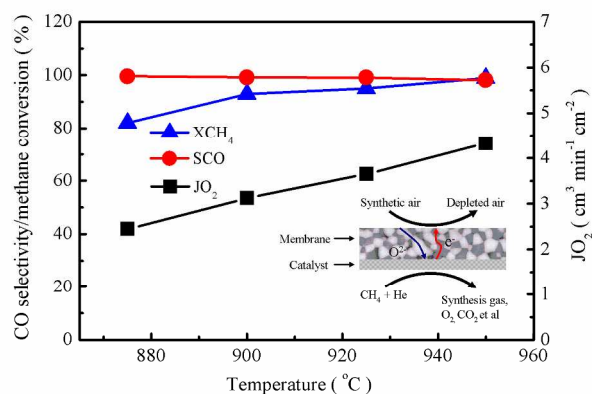


Fig. 7 Influence of temperature on the CH_4 conversion (\blacktriangle), CO selectivity (\bullet) and oxygen permeation flux (\blacksquare) through the 40NSFO-60CNO dual phase membrane without LSC coating on the air side in the POM to synthesis gas. Conditions: $150 \text{ cm}^3 \text{ min}^{-1}$ air as feed gas, $11 \text{ cm}^3 \text{ min}^{-1}$ He with $8.27 \text{ cm}^3 \text{ min}^{-1}$ CH_4 as sweep gas; $1 \text{ cm}^3 \text{ min}^{-1}$ Ne as internal standard gas. Membrane thickness: 0.6 mm .

Fig. 7 presents the temperature influence on the CH_4 conversion, CO selectivity and oxygen permeation flux through the 40NSFO-60CNO dual phase membrane in the POM to synthesis gas. It was observed that the oxygen permeation fluxes increased from 2.44 cm^3

$\text{min}^{-1} \text{ cm}^{-2}$ to $4.33 \text{ cm}^3 \text{ min}^{-1} \text{ cm}^{-2}$ and the methane conversion increased from 82.1% to 98.8% with increasing temperatures from $875 \text{ }^\circ\text{C}$ to $950 \text{ }^\circ\text{C}$ while the CO selectivity slightly decreased from 99.6% to 98.1% . This behavior is in good agreement with the observation in previous studies.^{8,33} The reasons for this behavior are explained as follows: (1) The increased oxygen permeation flux was due to the increase of the oxygen diffusion rate through the 40NSFO-60CNO membrane and the faster surface kinetics with increasing temperature. (2) Further, the increasing amount of permeated oxygen leads to the increase of the methane conversion. (3) The decrease of the CO selectivity with increasing temperature is ascribed to some excess oxygen in comparison to the amount of oxygen required for the stoichiometry of POM.

Fig. 8 shows the influence of the methane concentration in the feed on the CH_4 conversion, CO selectivity and oxygen permeation flux through the 40NSFO-60CNO dual phase membrane in the POM to synthesis gas at $950 \text{ }^\circ\text{C}$. As shown in Fig. 8, with increasing methane concentration, the methane conversion decreases from 99.9% to 92.1% while the CO selectivity increases from 97.4% to 99.6% and the oxygen permeation fluxes increases from $3.16 \text{ cm}^3 \text{ min}^{-1} \text{ cm}^{-2}$ to $5.06 \text{ cm}^3 \text{ min}^{-1} \text{ cm}^{-2}$ when the methane concentrations of the feed increases from 30% to 60% . This experimental finding can be explained as follows: (1) The increased oxygen permeation flux was due to the increased driving force for oxygen permeation with increasing methane concentration. (2) However, at high methane concentrations the oxygen flux is increased, but more methane is available than needed for the stoichiometric POM. Thus, the methane conversion is reduced. (3) The higher the methane concentration, the less CO is oxidized to CO_2 which results in a higher CO selectivity.

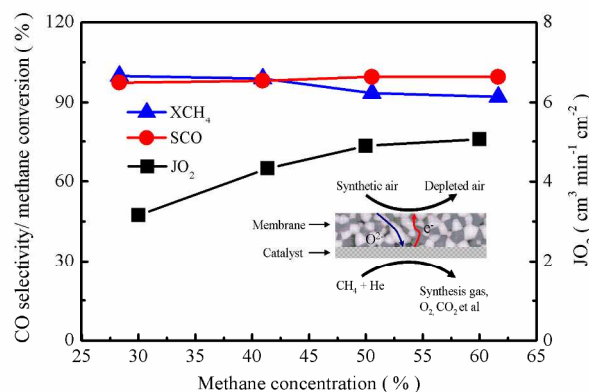


Fig. 8 Influence of methane concentration on the CH_4 conversion (\blacktriangle), CO selectivity (\bullet) and oxygen permeation flux (\blacksquare) through the 40NSFO-60CNO dual phase membrane without LSC coating on the air side in the POM to synthesis gas.

Conditions: Feed side: $F_{\text{air}} = 150 \text{ cm}^3 \text{ min}^{-1}$, Sweep side: $F_{\text{He}} + F_{\text{CH}_4} + F_{\text{Ne}} = 20 \text{ cm}^3 \text{ min}^{-1}$, $1 \text{ cm}^3 \text{ min}^{-1}$ Ne as internal standard gas, Membrane thickness: 0.6 mm . Temperature: $950 \text{ }^\circ\text{C}$

Conclusions

In this work, a novel dual phase oxygen transporting membrane with the composition $40\text{wt.}\% \text{ Nd}_{0.6}\text{Sr}_{0.4}\text{FeO}_{3-\delta}$ - $60\text{wt.}\% \text{ Ce}_{0.9}\text{Nd}_{0.1}\text{O}_{2-\delta}$ (40NSFO-60CNO) has been developed by using the in-situ EDTA-citric synthesis method. A stable

oxygen flux of $0.48 \text{ cm}^3 \text{ min}^{-1} \text{ cm}^{-2}$ can be achieved at $950 \text{ }^\circ\text{C}$ when using CO_2 as sweep gas for a 0.6 mm thick membrane with a porous $\text{La}_{0.6}\text{Sr}_{0.4}\text{CoO}_{3-\delta}$ (LSC) coating on the air side. The 40NSFO-60CNO membrane was stable for more than 150 h when using pure CO_2 as sweep gas. The 40NSFO-60CNO dual phase reactor was successfully performed for the POM to syngas. Methane conversion was found to be higher than 99.0% with 98.0% CO selectivity, a $4.33 \text{ cm}^3 \text{ min}^{-1} \text{ cm}^{-2}$ oxygen permeation flux was obtained under a steady state condition at $950 \text{ }^\circ\text{C}$. The results demonstrate that our 40NSFO-60CNO dual phase membrane is not only stable in CO_2 but also in reducing atmospheres, which is a promising membrane materials for the oxyfuel process for CO_2 capture. However, the oxygen permeation flux is lower than that of the industrial application requirement ($1 \text{ cm}^3 \text{ min}^{-1} \text{ cm}^{-2}$).⁴³ In future, further research need to improve the oxygen flux of this dual phase membrane by doping as well by technical measures such as an asymmetric membrane structures^{12,44,45} or by surface enlargement as demonstrated for a hollow fibre structure.⁴⁶

Acknowledgements

The authors acknowledge the financial support from the Sino-German Centre for Science Promotion (GZ 676, GZ911). H.H. Wang greatly acknowledges the financial support by National Science Fund for Distinguished Young Scholars of China (no. 21225625). The authors also greatly acknowledge F. Steinbach for technical support and Prof H. Jiang' useful discuss.

Notes and references

^a Institute of Physical Chemistry and Electrochemistry, Leibniz University of Hannover, Callinstr. 3A, D-30167 Hannover, Germany Fax: (49)511 762 19121; Tel: (49)511 762 3175; E-mail: juergen.caro@pci.uni-hannover.de

^b Department of Chemistry, Princeton University, Princeton, New Jersey 08544, USA. Town, Country. Fax: (01)609 258 6746; Tel: (01)609 258 5556; E-mail: huixial@princeton.edu

^c School of Chemistry & Chemical Engineering, South China University of Technology, No. 381 Wushan Road, 510640 Guangzhou, China Fax: (86)020 8711 0131; Tel: (86)020 8711 0131; E-mail: hhwang@scut.edu.cn

Electronic Supplementary Information (ESI) available: [details of any supplementary information available should be included here]. See DOI: 10.1039/b000000x/

- Z. P. Shao, S. M. Haile, J. Ahn, P. D. Ronney, Z. L. Zhan and S. A. Barnett, *Nature*, 2005, **435**, 795.
- Z. P. Shao and S. M. Haile, *Nature*, 2004, **431**, 170.
- H. Q. Jiang, H. H. Wang, F. Y. Liang, S. Werth, T. Schiestel and J. Caro, *Angew. Chem. Int. Ed.*, 2009, **48**, 2983.
- H. Q. Jiang, Z. W. Cao, S. Schirmermeister, T. Schiestel and J. Caro, *Angew. Chem. Int. Ed.*, 2010, **49**, 5656.
- Z. W. Cao, H. Q. Jiang, H. X. Luo, S. Baumann, W. A. Meulenber, J. Assmann, L. Mlecko, Y. Liu and J. Caro, *Angew. Chem. Int. Ed.*, 2013, **52**, 13794.
- X. Y. Tan, L. L. Shi, G. Z. Hao, B. Meng and S. M. Liu, *Sep. Purif. Technol.*, 2012, **96**, 89.
- H. X. Luo, K. Efimov, H. Q. Jiang, A. Feldhoff, H. H. Wang and J. Caro, *Angew. Chem. Int. Ed.*, 2011, **50**, 759.
- H. X. Luo, H. Q. Jiang, T. Klande, Z. H. Cao, F. Y. Liang, H. H. Wang and J. Caro, *Chem. Mater.*, 2012, **24**, 2148.
- S. M. Hashim, A. R. Mohamed and S. Bhatia, *Adv. Colloid Interface Sci.*, 2010, **160**, 88.
- V. M. Goldschmidt, *Die Naturwissenschaften*, 1926, **21**, 477.
- J. F. Vente, W. G. Haije and Z. S. Rak, *J. Membr. Sci.*, 2006, **276**, 178.
- S. Baumann, J.M. Serra, M. P. Lobera, S. Escolástico, F. Schulze-Küppers and W.A. Meulenber, *J. Membr. Sci.*, 2011, **377**, 198.
- H. Kruidhof, H. J. M. Bouwmeester, R. H. E. v. Doorn and A. J. Burggraaf, *Solid State Ionics*, 1993, **63-65**, 816.
- K. Efimov, Q. Xu and A. Feldhoff, *Chem. Mater.*, 2010, **22**, 5866.
- J. Kniep and Y. S. Lin, *Ind. Eng. Chem. Res.*, 2011, **50**, 7941.
- M. Arnold, T. M. Gesing, J. Martynczuk and A. Feldhoff, *Chem. Mater.*, 2008, **20**, 5851.
- M. Arnold, H. H. Wang and A. Feldhoff, *J. Membr. Sci.*, 2007, **293**, 44.
- O. Czuprat, M. Arnold, S. Schirmermeister, T. Schiestel and J. Caro, *J. Membr. Sci.*, 2010, **364**, 132.
- J. X. Yi, M. Schroeder, T. Weirich and J. Mayer, *Chem. Mater.*, 2010, **22**, 6246.
- H. X. Luo, H. Q. Jiang, K. Efimov, H. H. Wang and J. Caro, *AIChE J.*, 2011, **57**, 2738.
- H. X. Luo, H. Q. Jiang, K. Efimov, F. Y. Liang, H. H. Wang and J. Caro, *Ind. Eng. Chem. Res.*, 2011, **50**, 13508.
- H. X. Luo, H. Q. Jiang, T. Klande, F. Y. Liang, Z. W. Cao, H. H. Wang and J. Caro, *J. Membr. Sci.*, 2012, **423-424**, 450.
- X. F. Zhu, H. Y. Liu, Y. Cong and W. S. Yang, *Chem. Commun.*, 2012, **48**, 251.
- J. Xue, Q. Liao, Y. Y. Wei, Z. Li and H. H. Wang, *J. Membr. Sci.*, 2013, **443**, 124.
- Z. T. Wang, W. P. Sun, Z. W. Zhu, T. Liu and W. Liu, *ACS Appl. Mater. Interfaces*, 2013, **5**, 11038.
- T. Klande, O. Ravkina and A. Feldhoff, *J. Membr. Sci.* 2013, **437**, 122.
- A. A. Yaremchenko, V. V. Kharton, A. P. Viskup, E. N. Naumovich, V. N. Tikhonovich and N. M. Lapchuk, *Solid State Ionics*, 1999, **120**, 65.
- V. V. Kharton, A. V. Kovalevsky, M. V. Patrakeev, E. V. Tsipis, A. P. Viskup, V. A. Kolotygin, A. A. Yaremchenko, A. L. Shaula, E. A. Kiselev and J. o. C. Waerenborgh, *Chem. Mater.*, 2008, **20**, 6457.
- S. Omar, w, z E. D. Wachsman, J. L. Jones, and J. C. Nino, *J. Am. Ceram. Soc.*, 2009, **92**, 2674.
- http://en.wikipedia.org/wiki/Common-ion_effect
- H. X. Luo, B. B. Tian, Y. Y. Wei, H. H. Wang, H. Q. Jiang and J. Caro, *AIChE J.*, 2010, **56**, 604.
- Y. K. Tao, J. Shao, W. G. Wang, J. X. Wang, Fuel cells, 2009, **5**, 679.
- H. X. Luo, Y. Y. Wei, H. Q. Jiang, W. H. Yuan, Y. X. Lv, J. Caro and H. H. Wang, *J. Membr. Sci.*, 2010, **350**, 154.
- F. Y. Liang, H. X. Luo, K. Partovi, O. Ravkina, Z. W. Cao, Y. Liu and J. Caro, *Chem. Commun.*, 2014, **50**, 2451.
- X. F. Zhu, H.Y. Liu, Q. M. Li, Y. Cong, W. S. Cong, *Solid State Ionics*, 2011, **185**, 27.

- 36 H. B. Li, Y. Liu, X. F. Zhu, Y. Cong, S. P. Xu, W. Q. Xu and W. S. Yang, *Sep. Purif. Technol.*, 2013, **114**, 31.
- 37 S. W. Leea, K. S. Leeb, S. K. Woob, J. W. Kim, T. Ishiharad, D. K. Kim, *Solid State Ionics*, 2003, **158**, 287.
- 38 J. Sunarso, S. Baumann, J. M. Serra, W.A. Meulenber, S. Liu, Y.S. Lin, J.C. Diniz da Costa, *J. Membr. Sci.*, 2011, **377**, 198.
- 39 J. H. Tong, W. S. Yang, B. C. Zhu and R. Cai, *J. Membr. Sci.*, 2002, **203**, 175.
- 40 J. M. Serra, J. G. Fayos, S. Baumann, F. S. Küppers, W. A. Meulenber, *J. Membr. Sci.*, 2013, **447**, 297.
- 41 X. Y. Tan, N. Liu, B. Meng, J. Sunarso, K. Zhang, S. M. Liu, *J. Membr. Sci.*, 2012, **389**, 216.
- 42 K. Efimov, T. Klande, N. Judizki, A. Feldhoff, *J. Membr. Sci.*, 2012, **389**, 205.
- 43 B. C. H. Steele, *Curr. Opin. Solid State Mater. Sci.*, 1996, **1**, 684.
- 44 M. P. Lobera, J. M. nt, S. P Foghmoes, M. Sogaard, A. Kaiser, *J. Membr. Sci.* 2011, 385-386, 154.
- 45 A. Kaiser, S. Foghmoes, C. Chatzichristodoulou, M. Sogaard, J. A. Glasscock, H. L. Frandsen, P. V. Hendriksen, *J. Membr. Sci.* 2011, **378**, 51.
- 46 X. Y. Tan, Z. G. Wang, B. Meng, X. X. Meng, K. Li, *J. Membr. Sci.* 2010, **352**, 189.

Graphical Abstract

CO₂-stable reduction-tolerant Nd-containing dual phase membrane for oxyfuel CO₂ capture

Huixia Luo,^{a,b*} Tobias. Klande,^a Zhengwen Cao,^a Fangyi Liang,^a Haihui Wang,^{c*} and Jürgen Caro^{a*}

^a Institute of Physical Chemistry and Electrochemistry, Leibniz University of Hannover, Callinstr. 3A, D-30167 Hannover, Germany

^b Department of Chemistry, Princeton University, Princeton, New Jersey 08544, USA

^c School of Chemistry & Chemical Engineering, South China University of Technology, No. 381 Wushan Road, 510640 Guangzhou, China

We report a novel CO₂-stable reduction-tolerant dual-phase oxygen transport membrane 40 wt.% Nd_{0.6}Sr_{0.4}FeO_{3-δ}-60 wt.% Ce_{0.9}Nd_{0.1}O_{2-δ}. This membrane material shows a good reversibility of the oxygen permeation fluxes, good stability in a CO₂ atmosphere and under the harsh conditions of the partial oxidation of methane to synthesis gas up to 950 °C.

